PROCEEDINGS OF SCIENCE

Anisotropic flow of strange and multi-strange hadrons in Ru+Ru and Zr+Zr collisions at $\sqrt{s_{\rm NN}}$ = 200 GeV at RHIC

Vipul Bairathi (for the STAR Collaboration)[a,*]

[a] *Instituto de Alta Investigación, Universidad de Tarapacá, Casilla 7D, Arica 1000000, Chile*

E-mail: vipul.bairathi@gmail.com

We present elliptic flow of strange and multi-strange hadrons (K^0_s, Λ, $\bar{\Lambda}$, ϕ, Ξ^-, and $\bar{\Xi}^+$) at mid-rapidity in isobar collisions ($^{96}_{44}$Ru+$^{96}_{44}$Ru and $^{96}_{40}$Zr+$^{96}_{40}$Zr) at $\sqrt{s_{\rm NN}}$ = 200 GeV. The transverse momentum (p_T) dependence of elliptic flow (v_2) is presented for minimum bias and various collision centrality intervals. We studied the number of constituent quark (NCQ) scaling of v_2 in these isobar collisions. Average elliptic flow ($\langle v_2 \rangle$) has been observed to increase from central to peripheral collisions. The ratio of $\langle v_2 \rangle$ between isobar species shows a deviation from unity that is consistent with the difference in nuclear structure and deformation in these species. A system size dependence of v_2 is also observed among isobar, Cu+Cu, Au+Au, and U+U systems.

41st International Conference on High Energy physics - ICHEP2022
6-13 July, 2022
Bologna, Italy

*Speaker

1. Introduction

Several studies in relativistic heavy-ion collisions at the Relativistic Heavy Ion Collider (RHIC) [1–4] and the Large Hadron Collider (LHC) [5–7] suggest the formation of an exotic state of matter called the quark-gluon plasma (QGP) [8]. One of the key observables in these studies is azimuthal anisotropic flow of produced particles which indicates hydrodynamic and collective behavior of the strongly interacting matter during the collision. Such an observable measures the anisotropy in event-by-event azimuthal angle distribution of produced particles relative to the collision plane. It arises due to spatial anisotropy of the initial overlap geometry of the colliding nuclei as a consequence of inhomogeneous initial energy deposition and fluctuations of nucleon positions in heavy-ion collisions. The initial spatial anisotropies are converted into final state momentum anisotropies through strong rescatterings among partons during the early stages prior to hadronization, and among produced hadrons at the later stages. The anisotropic flow is an important tool to explore the properties of the QGP matter formed in the relativistic heavy-ion collisions.

2. Data analysis

In the year 2018, the STAR experiment at RHIC collected data by colliding isobar species Ru+Ru and Zr+Zr at $\sqrt{s_{\rm NN}}$ = 200 GeV. It is dedicated to measure the charge separation along the magnetic field, driven by a phenomenon called the Chiral Magnetic Effect (CME) [9]. It was realized that the two isobars have different deformation parameters and flow measurements are highly sensitive to them. More importantly, measurements of strange and multi-strange hadrons flow is an excellent probe for understanding the initial state anisotropies due to their small hadronic interaction cross-section compared to light hadrons. Therefore, a systematic study of anisotropic flow of strange and multi-strange hadrons could be crucial to understand the effect of initial states in the isobar collisions.

Anisotropic flow is quantified via the Fourier decomposition of the particle azimuthal angle distribution with respect to the event plane angle. The azimuthal dependence of the particle yield can be expanded in terms of a Fourier series [10]:

$$E\frac{d^3N}{dp^3} = \frac{d^2N}{2\pi p_T dp_T dy}\left(1 + 2\sum_{n=1}^{\infty} v_n(p_T, y)\cos[n(\phi - \Psi_n)]\right), \quad (1)$$

where ϕ, p_T, and y are the particle's azimuthal angle, transverse momentum, and rapidity, respectively, and Ψ_n is the orientation of the nth-order event plane. The second order Fourier coefficient v_2, known as elliptic flow, is particularly sensitive to the initial geometry of the collisions and the properties of the medium in the heavy-ion collisions.

In these proceedings, we report v_2 of K^0_s, Λ, $\bar{\Lambda}$, ϕ, Ξ^-, and $\overline{\Xi}^+$ in Ru+Ru and Zr+Zr collisions at $\sqrt{s_{\rm NN}}$ = 200 GeV. A total of ~650 M minimum bias good events out of the total 1.8 B (2 B) events of Ru+Ru (Zr+Zr) collisions are used for this analysis. The above hadrons are reconstructed using the invariant mass technique through their hadronic decay channels. The combinatorial background is constructed using a track rotation method for weakly decaying hadrons, while for ϕ-mesons event mixing technique is used [11, 12]. The

η-sub event plane method with a η-gap of 0.1 between the two sub-events (-1 < η < -0.05 and 0.05 < η < 1.0) has been used to calculate v_2 of these hadrons [10].

3. Results

3.1 p_T dependence of v_2

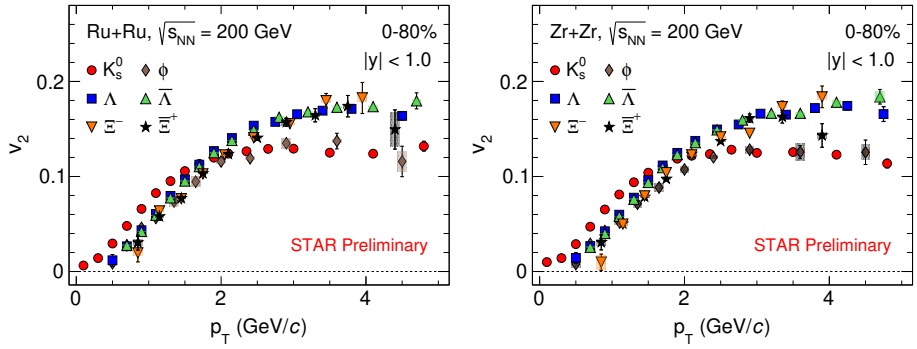

Figure 1: v_2 as a function of p_T for strange and multi-strange hadrons at mid-rapidity in minimum bias Ru+Ru collisions (left panel) and Zr+Zr collisions (right panel) at $\sqrt{s_{\rm NN}}$ = 200 GeV.

Figure 1 shows p_T dependence of strange and multi-strange hadrons v_2 for minimum bias Ru+Ru and Zr+Zr collisions at $\sqrt{s_{\rm NN}}$ = 200 GeV. At low p_T, v_2 follows a particle mass dependence, indicating hydrodynamic behavior of the medium but interestingly at intermediate p_T, v_2 follows the particle type dependence (baryon vs meson) which suggests the formation of a QGP medium in the isobar collisions at $\sqrt{s_{\rm NN}}$ = 200 GeV. The same particle mass and type dependence of v_2 is observed for all the other centrality intervals.

3.2 Centrality dependence of v_2

Figures 2 and 3 show $v_2(p_T)$ of strange and multi-strange hadrons for various centrality intervals in Ru+Ru and Zr+Zr collisions at $\sqrt{s_{\rm NN}}$ = 200 GeV. A clear centrality dependence is observed for all the measured particle species in both the isobar collisions. The v_2 magnitude increases from central to peripheral collisions.

Figure 4 shows p_T-integrated v_2 of strange hadrons as a function of centrality in Ru+Ru and Zr+Zr collisions at $\sqrt{s_{\rm NN}}$ = 200 GeV. The ratio of v_2 in Ru+Ru to Zr+Zr collisions is also shown in the bottom panels of Fig. 4 and fitted with a constant polynomial function for mid-central collisions (20-50%). About ~2% deviation from unity with a significance of 6.25σ for $\Lambda(\bar{\Lambda})$ and 1.83σ for K^0_s is observed, which is consistent with the expectation from the difference between the nuclear structures of the two isobar nuclei [9].

3.3 NCQ scaling

Figure 5 shows v_2 of strange and multi-strange hadrons scaled by the number of constituent quarks n_q in minimum bias Ru+Ru and Zr+Zr collisions at $\sqrt{s_{\rm NN}}$ = 200 GeV. The results are presented as a function of transverse kinetic energy to remove the effect of particle mass at low p_T. It is defined as $KE_T = m_T - m_0$, where m_T is the transverse

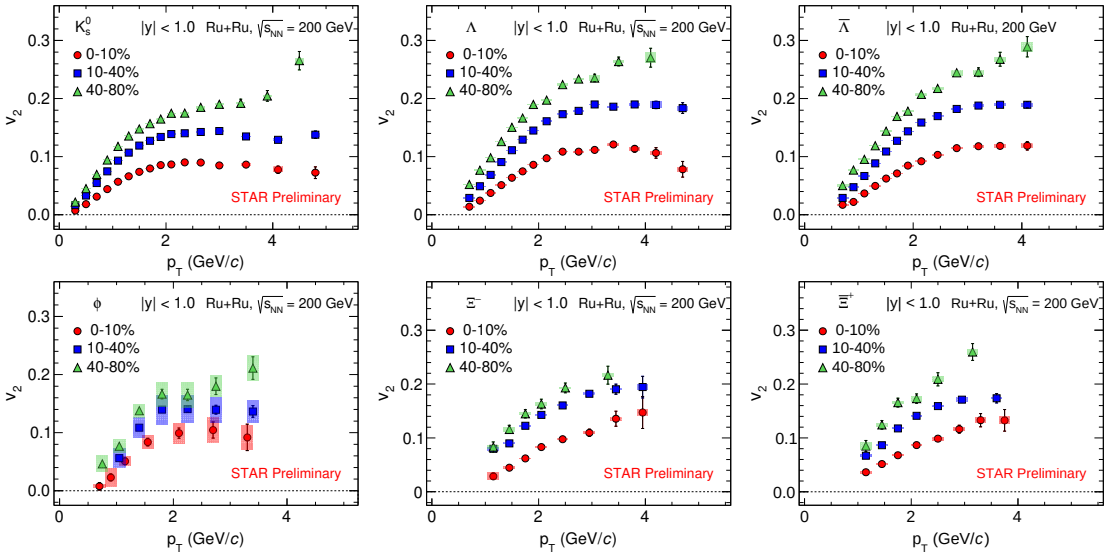

Figure 2: $v_2(p_T)$ of strange and multi-strange hadrons at mid-rapidity in Ru+Ru collisions at $\sqrt{s_{\rm NN}}$ = 200 GeV for centrality 0-10%, 10-40%, and 40-80%.

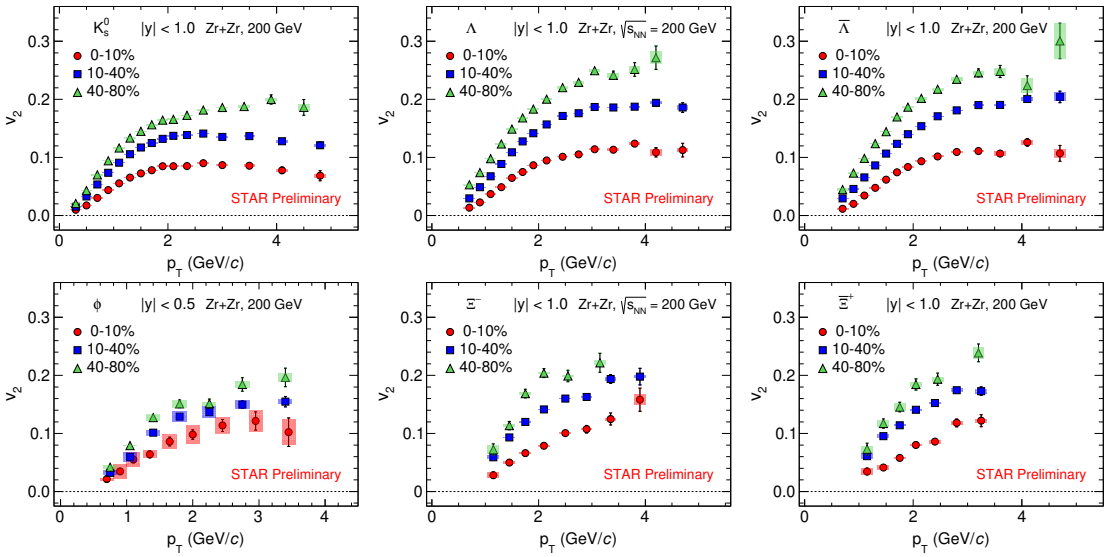

Figure 3: $v_2(p_T)$ of strange and multi-strange hadrons at mid-rapidity in Zr+Zr collisions at $\sqrt{s_{\rm NN}}$ = 200 GeV for centrality 0-10%, 10-40%, and 40-80%.

mass ($\sqrt{p_T^2 + m_0^2}$) and m_0 is rest mass of the particle. The v_2 of strange and multi-strange hadrons follows the number of constituent quarks (NCQ) scaling in both the collision systems. The NCQ scaling of v_2 suggests a formation and collective behavior of the QGP medium. It also indicates that the quark coalescence is the dominant mechanism of particle production.

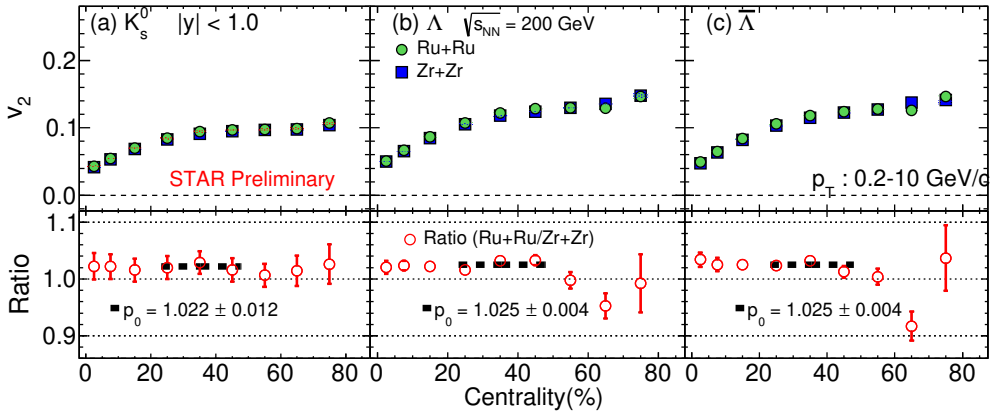

Figure 4: p_T-integrated v_2 vs centrality for strange hadrons at mid-rapidity in Ru+Ru and Zr+Zr collisions at $\sqrt{s_{\rm NN}}$ = 200 GeV. The ratio of v_2 between Ru and Zr is also shown in the bottom panels. The error bars represent statistical and systematic uncertainties added in quadrature.

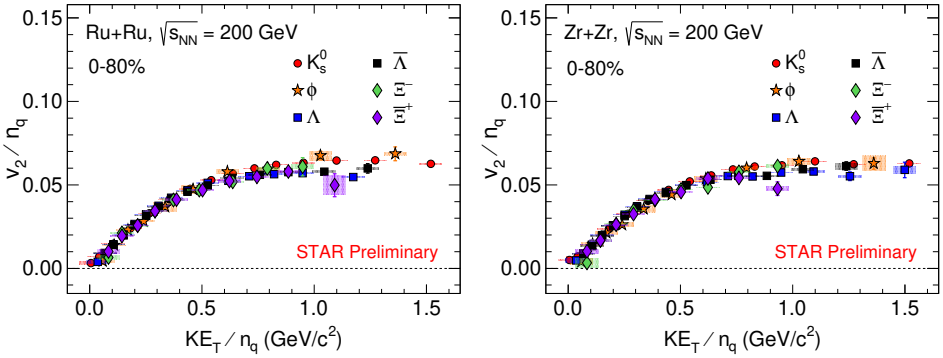

Figure 5: NCQ scaled v_2 vs transverse kinetic energy (KE_T/n_q) at mid-rapidity in minimum bias Ru+Ru and Zr+Zr collisions at $\sqrt{s_{\rm NN}}$ = 200 GeV. The bands represent systematic uncertainties.

3.4 System size dependence

Figure 6 shows v_2 of strange hadrons in Ru+Ru and Zr+Zr collisions at $\sqrt{s_{\rm NN}}$ = 200 GeV compared to the published results from the STAR experiment at RHIC in Cu+Cu, Au+Au, and U+U collisions [13–15]. A system size dependence of v_2 is observed for p_T above ∼1.5 GeV/c. The v_2 seems to follow the hierarchy $v_2^{\rm Cu} < v_2^{\rm Ru/Zr} < v_2^{\rm Au} < v_2^{\rm U}$. Its magnitude increases with increase in the system size.

4. Summary

We reported transverse momentum dependence of elliptic flow of K^0_s, Λ, $\bar{\Lambda}$, ϕ, Ξ^-, and $\bar{\Xi}^+$ in Ru+Ru and Zr+Zr collisions at $\sqrt{s_{\rm NN}}$ = 200 GeV for minimum bias (0-80%) and in three centrality intervals (0-10%, 10-40%, and 40-80%). A clear centrality dependence of v_2 is observed in the isobar collisions. We observed a particle mass hierarchy of v_2 which suggests hydrodynamic behavior at low p_T. A baryon-meson splitting at intermediate p_T suggests particle type dependence of v_2. Elliptic flow of strange and multi-strange hadrons follows the NCQ scaling, further indicating quark coalescence as the dominant particle

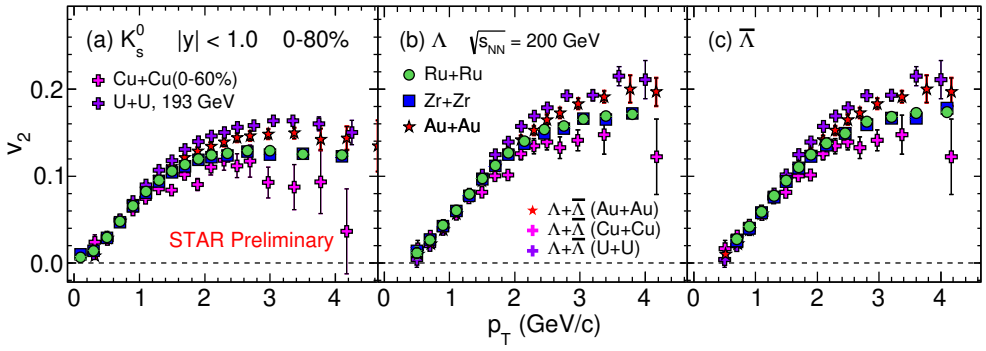

Figure 6: Strange hadron v_2 as a function of p_T at mid-rapidity in minimum bias Ru+Ru and Zr+Zr collisions at $\sqrt{s_{\rm NN}}$ = 200 GeV compared to Cu+Cu, Au+Au, and U+U collisions [13–15]. The error bars represent statistical and systematic uncertainties added in quadrature.

production mechanism and the collectivity of the medium. Ratio of p_T-integrated v_2 for strange hadrons between the two isobar collisions shows a deviation from unity. We also observed a system size dependence of the v_2. These measurements could shed light on the effect of deformation and collision geometry on anisotropic particle production in relativistic heavy-ion collisions.

References

[1] I. Arsene *et al.*, Nucl. Phys. A **757**, 1-27 (2005).

[2] B. B. Back *et al.*, Nucl. Phys. A **757**, 28-101 (2005).

[3] J. Adams *et al.*, Nucl. Phys. A **757**, 102-183 (2005).

[4] K. Adcox *et al.*, Nucl. Phys. A **757**, 184-283 (2005).

[5] K. Aamodt *et al.*, Phys. Rev. Lett. **105**, 252302 (2010).

[6] S. Chatrchyan *et al.*, Phys. Lett. B **707**, 330-348 (2012).

[7] G. Aad *et al.*, Phys. Rev. C **87**, 014902 (2013).

[8] S. A. Bass *et al.*, J. Phys. G **25**, R1-R57 (1999).

[9] M. S. Abdallah *et al.*, Phys. Rev. C **105**, 14901 (2022).

[10] A. M. Poskanzer and S. A. Voloshin, Phys. Rev. C **58**, 1671 (1998).

[11] J. Adams *et al.*, Phys. Rev. Lett. **95**, 122301 (2005).

[12] L. Adamczyk *et al.*, Phys. Rev. C **88**, 014902 (2013).

[13] B. I. Abelev *et al.*, Phys. Rev. C **77**, 054901 (2008).

[14] B. I. Abelev *et al.*, Phys. Rev. C **81**, 044902 (2010).

[15] M. S. Abdallah *et al.*, Phys. Rev. C **103**, 064907 (2021).